Mycobacterium tuberculosis Lipoamide Dehydrogenase Is Encoded by Rv0462 and Not by the *lpdA* or *lpdB* Genes†

Argyrides Argyrou and John S. Blanchard*

Department of Biochemistry, Albert Einstein College of Medicine, 1300 Morris Park Avenue, Bronx, New York 10461

Received March 21, 2001; Revised Manuscript Received July 23, 2001

ABSTRACT: The gene encoding dihydrolipoamide dehydrogenase from *Mycobacterium tuberculosis*, Rv0462, was expressed in *Escherichia coli* and the protein purified to homogeneity. The 49 kDa polypeptide forms a homodimer containing one tightly bound molecule of FAD/monomer. The results of steady-state kinetic analyses using several reduced pyridine nucleotide analogs and a variety of electron acceptors, and the ability of the enzyme to catalyze the transhydrogenation of NADH and thio-NAD^+ in the absence of D,L-lipoamide, demonstrated that the enzyme uses a ping−pong kinetic mechanism. Primary deuterium kinetic isotope effects on V and V/K at pH 7.5 using NADH deuterated at the C_4-*proS* position of the nicotinamide ring are small [$^D(V/K)_{NADH} = 1.12 \pm 0.15$, $^DV_{app} = 1.05 \pm 0.07$] when D,L-lipoamide is the oxidant but large and equivalent [$^D(V/K)_{NADH} = {}^DV = 2.95 \pm 0.03$] when 5-hydroxy-1,4-naphthoquinone is the oxidant. Solvent deuterium kinetic isotope effects at pH 5.8, using APADH as the reductant, are inverse with $^D(V/K)_{APADH} = 0.73 \pm 0.03$, $^D(V/K)_{Lip(S)_2} = 0.77 \pm 0.03$, and $^DV_{app} = 0.77 \pm 0.01$. Solvent deuterium kinetic isotope effects with 4,4-dithiopyridine (DTP), the 4-thiopyridone product of which requires no protonation, are also inverse with $^D(V/K)_{APADH} = 0.75 \pm 0.06$, $^D(V/K)_{DTP} = 0.71 \pm 0.02$, and $^DV_{app} = 0.56 \pm 0.15$. All proton inventories were linear, indicating that a single proton is being transferred in the solvent isotopically sensitive step. Taken together, these results suggest that (1) the reductive half-reaction (hydride transfer from NADH to FAD) is rate limiting when a quinone is the oxidant, and (2) deprotonation of enzymic thiols, most likely Cys_{46} and Cys_{41}, limits the reductive and oxidative half-reactions, respectively, when D,L-lipoamide is the oxidant.

The pyridine nucleotide:disulfide oxidoreductases form a family of flavoproteins which share many structural and mechanistic properties (*1*). Members of this family include dihydrolipoamide dehydrogenase, glutathione reductase, mycothione reductase, trypanothione reductase, and mercuric reductase, all of which perform critical metabolic and cellular functions. These enzymes catalyze the reduction of a disulfide-bonded substrate (or mercuric ion) using reducing equivalents from NADH or NADPH. For example, dihydrolipoamide dehydrogenase catalyzes the reversible reduction of lipoamide to dihydrolipoamide using reducing equivalents from NADH (eq 1).

$$NADH + H^+ + Lip(S)_2 \rightleftharpoons NAD^+ + Lip(SH)_2 \quad (1)$$

Dihydrolipoamide dehydrogenase (NADH:lipoamide oxidoreductase, EC 1.8.1.4) comprises the E3 component of the pyruvate dehydrogenase, α-ketoglutarate dehydrogenase, and glycine reductase multienzyme complexes (*2*). In vivo, it catalyzes the NAD^+-dependent oxidation of the dihydrolipoyl cofactors (reverse reaction of eq 1) that are covalently linked to the acyltransferase (E2) components of these multienzyme complexes.

The pyridine nucleotide:disulfide oxidoreductases are homodimers containing a single molecule of tightly bound FAD/monomer (*1*). At the amino acid sequence level, the binding motif for the ADP portion (GXGXXG, where X is any amino acid) of FAD (*3*) is readily identifiable near the N-terminus of the polypeptide chain (Figure 1). They also contain a redox-active disulfide formed between two cysteine residues (Cys^N and Cys^C)[1] separated by four amino acids, also located near the N-terminus of the polypeptide chain. The binding motif for the ADP portion (GXGXXG) of NADH is located roughly in the middle of the protein. Finally, an essential His-Glu pair located at the C-terminus of the adjacent monomer of the dimeric protein mediates proton transfer between enzymic and substrate thiolates/thiols.

A search of the annotated, completed sequence of the *Mycobacterium tuberculosis* H37Rv genome, revealed five

† Supported by NIH Grant GM33449.

* To whom correspondence should be addressed. Phone: (718) 430-3096. Fax: (718) 430-8565. E-mail: blanchar@aecom.yu.edu.

[1] Abbreviations: APADH, 3-acetylpyridine adenine dinucleotide; ATP, adenosine 5′-triphosphate; Cys^N and Cys^C, N- and C-terminal cysteine residues (Cys_{41} and Cys_{46} in the Rv0462 open reading frame) comprising the redox-active disulfide; DCPIP, 2,6-dichlorophenolindophenol; DTP, 4,4-dithiopyridine; D_2O, deuterium oxide; DMBQ, 2,6-dimethyl-1,4-benzoquinone; FAD, flavin adenine dinucleotide; HEPES, *N*-(2-hydroxyethyl)piperazine-*N*′-(2-ethanesulfonic acid); 5-HNQ, 5-hydroxy-1,4-naphthoquinone; IPTG, isopropyl-1-thio-β-D-galactopyranoside; $Lip(S)_2$, oxidized lipoamide; $Lip(SH)_2$, dihydrolipoamide (reduced lipoamide); MES, 2-(*N*-morpholino)ethanesulfonic acid; NADH, β-nicotinamide adenine dinucleotide; NADPH, β-nicotinamide adenine dinucleotide phosphate; tNADH, thio-nicotinamide adenine dinucleotide; NHDH, nicotinamide hypoxanthine dinucleotide; *orf*(*s*), open-reading frame(s); PCR, polymerase chain reaction; SDS−PAGE, sodium dodecyl sulfate−polyacrylamide gel electrophoresis; TEA, triethanolamine.

10.1021/bi010575o CCC: $20.00
Published on Web 08/30/2001

A

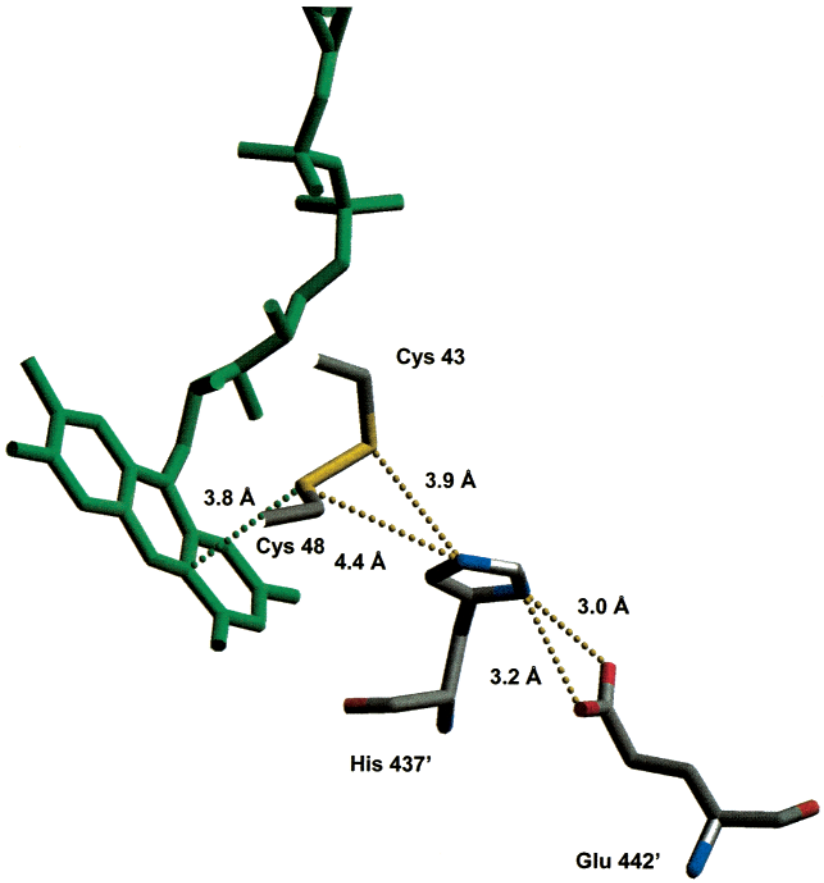

B

Gene	*Motif I*	*Motif II*	*Motif III*	*Motif IV*	*% Identical*	*% Similar*
E. coli lpd	^{13}GAGPAG^{18}	^{46}CLNVGC^{51}	^{184}GGGIIG^{189}	^{450}HPTLHE^{455}	100	100
M. tuberculosis lpdC	GAGPGG	CLNVGC	GAGAIG	HPTMSE	37	48
M. tuberculosis gorA	GTGSGN	CLNVGC	GSGFIA	HPALPE	30	42
M. tuberculosis lpdA	GGGPAG	AVLDDC	GSGVTG	YPSLSG	26	38
M. tuberculosis lpdB	GAGPVG	CSYWAC	GAGGVG	FPTISE	27	38
M. tuberculosis Rv2713	GSGPGG	CVNTGT	GAGVIG	YPTFSE	33	43

FIGURE 1: (A) Active site of lipoamide dehydrogenase from *Pseudomonas putida* illustrating the arrangement of catalytic residues relative to the bound FAD cofactor (*34*). Primed numbers indicate amino acids of the adjacent monomer of the dimer. (B) Comparison of amino acid sequence alignments of catalytic residues (motifs II and IV), FAD (motif I), and NADH (motif III) binding motifs of the five *orfs* in *M. tuberculosis* and the *E. coli* dihydrolipoamide dehydrogenase (*lpd*).

open-reading frames (*orfs*) of ~50 kDa in size, with significant amino acid sequence identity to the above enzyme family: *lpdA* (Rv3303c), *lpdB* (Rv0794c), *gorA* (Rv2855), Rv0462, and Rv2713. Pairwise comparisons of these *orfs* with the *Escherichia coli* dihydrolipoamide dehydrogenase amino acid sequence show 26−37% sequence identity and 38−48% similarity (Figure 1B). All sequences contain the FAD and pyridine nucleotide binding motifs (above and Figure 1), but not all contain the conserved cysteine residues nor the conserved His-Glu pair. Given the functional importance of this enzyme family, we have undertaken to clone and purify the proteins encoded by these genes and to structurally and functionally characterize them. This laboratory has previously shown that the gene annotated as *gorA* codes for a flavoprotein reductase that reduces mycothione to mycothiol (*4*). Mycothiol is an abundant, low molecular weight thiol, present in *M. tuberculosis* and other actinomycetes, that is thought to be functionally equivalent to reduced glutathione in oxidative stress management (*5*). The *lpdA* and *lpdB* genes have been designated as probable dihydrolipoamide dehydrogenases (*6*) (thus the designation, *lpd*). We have cloned and purified the protein encoded by *lpdA*, following expression in *E. coli*, and showed that it cannot reduce D,L-lipoamide, but it can reduce nonspecific substrates such as quinones and cytochrome *c* using reducing equivalents from NADH or NADPH (A.A. and J.S.B., unpublished results). The *lpdB* and Rv2713 gene products are unlikely to have dihydrolipoamide dehydrogenase activity since they lack the essential histidine residue near the C-terminus of the enzyme and, in addition, Rv2713 lacks Cys^{C}. The most likely candidate for the *M. tuberculosis* dihydrolipoamide dehydrogenase is the protein encoded by the Rv0462 gene, which so far has not been functionally annotated. It is 35−43% identical in amino acid sequence

to the kinetically (*E. coli* and pig) and structurally characterized (*Azotobacter vinelandii*, *Pseudomonas fluorescens*, and *Pseudomonas putida*) dihydrolipoamide dehydrogenases and contains all essential catalytic residues, as well as the two nucleotide binding motifs.

In this paper, we describe the cloning of Rv0462 and purification of the protein product following expression in *E. coli*. We show that it indeed encodes dihydrolipoamide dehydrogenase. We have, thus, termed the gene *lpdC*. We describe its physicochemical properties, substrate specificity, and steady-state kinetic mechanism. We have also probed the nature of the rate-limiting steps using steady-state primary deuterium and solvent kinetic isotope effects.

EXPERIMENTAL PROCEDURES

Materials. All chemicals were of analytical or reagent grade and were used without further purification unless otherwise stated. D,L-Lipoamide, D,L-lipoic acid, NADH, NAD^+, tNADH, $tNAD^+$, APADH, NHDH, ATP, glucose-6-phosphate dehydrogenase from *Leuconostoc mesenteroides* (type XXIV), and yeast hexokinase (type C-300) were from Sigma. 5-HNQ, DMBQ, D-glucose-1-*d* (97% atom D), and DTP were from Aldrich. D_2O (>99.8 atom % D) was from Cambridge Isotope Laboratories. All restriction enzymes and T4 DNA ligase were obtained from New England Biolabs.

General Methods. Protein concentrations were determined with bicinchoninic acid (*7*) using bovine serum albumin as standard. Solution pH values were measured at 25 °C with an Accumet model 20 pH meter and Accumet combination electrode standardized at pH 7.00 and 4.00 or 10.00. Spectrophotometric assays were performed using a UVIKON 943 double beam UV−VIS spectrophotometer.

Cloning and Expression of M. tuberculosis Dihydrolipoamide Dehydrogenase. The gene encoding dihydrolipoamide dehydrogenase (Rv0462, *lpdC*) from *M. tuberculosis* was identified as described in the introductory portion of this paper. The gene was amplified by PCR to generate blunt-ended DNA with *Nde*I and *Bam*HI restriction sites at the ends, using two oligonucleotide primers (5′-ATTCCATATGACCCACTATGACGTCGTC-3′ and 5′-CGCGGATCCTCAGAAATTGATCATGTGGCC-3′) complimentary to the amino-terminal coding and carboxyl-terminal noncoding strands of this gene, *M. tuberculosis* H37Rv genomic DNA, and *Pfu* DNA polymerase (Stratagene). The amplified DNA product was ligated into the pCR-Blunt plasmid and transformed into One Shot TOP10 cells following the instructions supplied by the manufacturer (Invitrogen). Plasmid DNA isolated from these cells was then digested with *Nde*I and *Bam*HI and the purified insert was ligated into purified plasmid pET-23a(+) (Novagen) previously linearized with the same restriction enzymes. This recombinant plasmid was then transformed into competent *E. coli* BL21 (DE3) cells (Novagen). The BL21 (DE3) cells containing pET23a(+): *lpdC* were grown at 37 °C to an A_{600nm} of 0.7 in Luria-Bertani medium containing 50 μg/mL ampicillin. The cells were then cooled to 20 °C, the temperature was equilibrated for 2 h, and the induction of protein expression by the addition of 1mM IPTG was allowed to proceed for 12 h at 20 °C. DNA sequencing of the cloned *lpdC* gene showed that it was free of mutations.

Purification of Dihydrolipoamide Dehydrogenase. All operations were carried out at 4 °C. Cell paste (63 g) was suspended in 40 mL of 20 mM TEA, pH 7.8, containing three tablets of Complete protease inhibitor cocktail (Boehringer Mannheim), 22 mg of chicken egg white lysozyme (Sigma), 9 mg of bovine pancreas DNaseI (Boehringer Mannheim), and 10 mM $MgCl_2$ and stirred for 30 min. The cells were disrupted by sonication, and cell debris was removed by centrifugation at 20000*g* for 70 min. The supernatant was dialyzed for 4 h against 4 L of 20 mM TEA, pH 7.8, and the precipitate which formed during dialysis was removed by centrifugation as above. The dialysate (110 mL) was applied to a 100 mL column of Q-Sepharose FF (Amersham-Pharmacia Biotech) equilibrated with 20 mM TEA, pH 7.8. The column was washed with 200 mL of the same buffer and then eluted with a linear gradient (1000 mL) from 0 to 1 M NaCl in 20 mM TEA, pH 7.8. The yellow fractions containing dihydrolipoamide dehydrogenase, which eluted at ~0.58 M NaCl, were pooled (56 mL), dialyzed against 4 L of 20 mM TEA, pH 7.8, for 5 h and solid $(NH_4)_2SO_4$ was added to a final concentration of 1 M. The supernatant, after centrifugation as above, was then applied to a 75 mL column of Phenyl-Sepharose HP (Amersham-Pharmacia Biotech) equilibrated with 20 mM TEA, pH 7.8, containing 1 M $(NH_4)_2SO_4$. The column was washed with 200 mL of the same buffer and then eluted with a linear reverse gradient (800 mL) from 1 to 0 M $(NH_4)_2SO_4$. Dihydrolipoamide dehydrogenase eluted in two peaks. Peak I, which eluted at ~ 410 mM $(NH_4)_2SO_4$, had a protein to FAD ratio of 1.21 while peak II, which eluted at ~70 mM $(NH_4)_2SO_4$, had a protein to FAD ratio of 2.51. Both peaks were >95% pure. Electrospray ionization/mass spectrometry showed a subunit molecular mass of 49 231 Da (peak I) and 49 233 Da (peak II) consistent with the molecular mass of 49 237 Da predicted from the amino acid sequence of *M. tuberculosis lpdC*. Peak I had a specific dihydrolipoamide dehydrogenase activity twice that of peak II. Addition of 1 mM FAD in 20 mM TEA, pH 7.8, containing 1 M $(NH_4)_2SO_4$ to peak II resulted in the complete conversion of peak II to peak I protein. Gel filtration chromatography of both peaks was carried out on a 320 mL calibrated HiTrap Sephacryl S-200 HR column (Amersham-Pharmacia Biotech) using 50 mM Hepes, pH 7.5, containing 150 mM NaCl as the elution buffer. Both peaks eluted as dimers. A total of 150 mg of pure protein was obtained from 63 g (12 L) of cell paste. All experiments reported in this paper were carried out using the same preparation of peak I protein. The enzyme concentration was determined from $\epsilon_{458nm} = 11\,300\ M^{-1}\ cm^{-1}$, and velocities (below) are based on enzyme monomers. The concentration of enzyme determined using a protein assay (see General Methods) with bovine serum albumin as standard agrees favorably (only 20% higher) with the value obtained using the above extinction coefficient.

Preparation of [4S-^{2}H]-NADH. 4S-Deuterated NADH was prepared by enzymatic reduction of the oxidized nucleotide with *Leuconostoc mesenteroides* (type XXIV) glucose-6-phosphate dehydrogenase using [1-^{2}H]-glucose-6-phosphate as the deuterium source as described previously (*8*). [*4S*-^{2}H]-NADH and nondeuterated NADH were purified on a Mono-Q column (Amersham-Pharmacia Biotech) as described previously (*9*), and the fractions with absorbance ratios $A_{260nm}/A_{340nm} \leq 2.3$ were pooled. The concentration of [*4S*-^{2}H] NADH and nondeuterated NADH was determined by enzymatic end-point assays with rabbit muscle L-lactate

dehydrogenase (type II, Sigma) in the presence of excess (5 mM) sodium pyruvate.

Assays for Dihydrolipoamide Dehydrogenase. All assays were performed at 25 °C under initial rate conditions. The NADH-dependent reduction of D,L-lipoamide, D,L-lipoic acid, quinones, and molecular oxygen catalyzed by dihydrolipoamide dehydrogenase was assayed spectrophotometrically at 340 nm ($\epsilon = 6220\ M^{-1}\ cm^{-1}$) associated with the oxidation of NADH. Assays contained 100 mM HEPES, pH 7.5, 1 mM EDTA, and 5% (v/v) methanol (for D,L-lipoamide and D,L-lipoic acid) or 1% (v/v) acetonitrile (for quinones and DTP). The oxidation of pyridine nucleotide analogs was monitored at the following wavelengths with the following extinction coefficients: tNADH (398 nm, $\epsilon = 11\ 300\ M^{-1}\ cm^{-1}$), NHDH (376 nm, $\epsilon = 1284\ M^{-1}\ cm^{-1}$), APADH (362 nm, $\epsilon = 9100\ M^{-1}\ cm^{-1}$ or 410 nm, $\epsilon = 1042\ M^{-1}\ cm^{-1}$). The reduction of DTP was monitored at 324 nm ($\epsilon = 19\ 800\ M^{-1}\ cm^{-1}$). Stock solutions of water-insoluble substrates were made in the following solvents: D,L-lipoamide and D,L-lipoic acid (50 mM) in methanol, DMBQ and 5-HNQ (50 mM) in acetonitrile, and DTP (200 mM) also in acetonitrile.

Solvent Isotope Effects. Solvent isotope effects were determined in 1 mL cuvettes. Seventy-five μL of 1.33 M MES, pH 5.8, was diluted with 900 μL of H_2O or D_2O to a final concentration of 100 mM. Substrates, enzyme, and EDTA (all in H_2O) made up the remaining 25 μL of the 1 mL reaction. Solvent isotope effects were performed in 100% H_2O or 90% D_2O and were corrected for incomplete deuteration using eq 4 (below). The proton inventories were performed in a similar manner by adjusting the H_2O to D_2O ratios.

Data Analysis. Data were fitted to the nonlinear least-squares curve-fitting programs of SigmaPlot version 3.0 (Jandel). Individual saturation curves were fitted to eq 2:

$$v = VA/(A + K) \quad (2)$$

where V is the maximal velocity, A is the substrate concentration, and K is the Michaelis constant (K_m). Data showing parallel initial velocity patterns on reciprocal plots were fitted to eq 3:

$$v = VAB/(K_AB + K_BA + AB) \quad (3)$$

where A and B and K_A and K_B are the concentrations and Michaelis constants, respectively, for the substrates. Primary and solvent deuterium kinetic isotope effects were calculated from eqs 4 and 5:

$$v = VA/[K(1 + F_iE_{V/K}) + A(1 + F_iE_V)] \quad (4)$$

$$v = VA/[(K + A)(1 + F_iE_V)] \quad (5)$$

where isotope effects exhibited on V and V/K are different or equivalent, respectively. F_i is the fraction of isotopic label, and $E_{V/K}$ and E_V are the isotope effects minus 1 on V/K and V, respectively. All values of the isotope effects were obtained from eq 4 except for the primary kinetic isotope effects in Figure 4B; in this case, eq 5 gave lower standard errors of the fitted parameters than eq 4.

RESULTS

Rv0462 Codes for Dihydrolipoamide Dehydrogenase. The gene (Rv0462, *lpdC*) encoding the *M. tuberculosis* dihydrolipoamide dehydrogenase was identified as described in the introductory portion of this paper. We cloned this gene into plasmid pET-23a(+) and overexpressed the protein in *E. coli* BL21 (DE3) cells. Induction of protein expression with 1 mM IPTG was performed at 20 °C, because the cells expressed more soluble protein at this lower temperature than at 37 °C. Column chromatography on Q-Sepharose FF followed by Phenyl Sepharose HP was sufficient to achieve homogeneity (Experimental Procedures). A single 50 kDa band was observed on an SDS−PAGE gel. Electrospray ionization/mass spectrometry and N-terminal sequence analysis confirmed the identity and integrity of the purified protein (Experimental Procedures). About 150 mg of pure soluble protein was obtained from 63 g of cell paste.

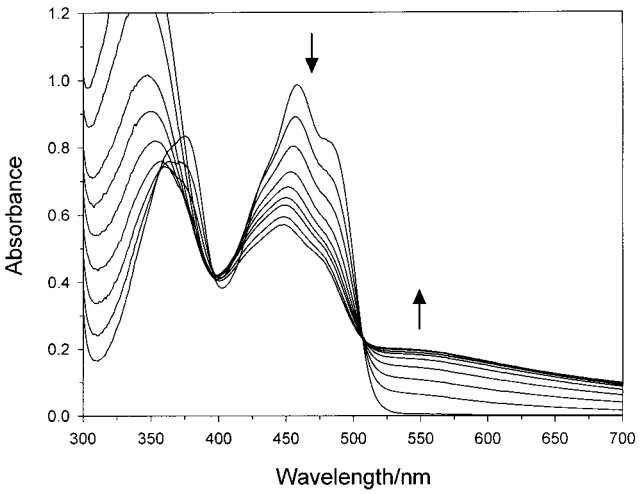

FIGURE 2: Anaerobic titration of *M. tuberculosis* dihydrolipoamide dehydrogenase with NADH in 85 mM Hepes, pH 7.5, 20% glycerol, at 25 °C. The uppermost spectrum at 458 nm is that of 88 μM (refers to FAD) oxidized enzyme (E_{OX}). The remaining are spectra recorded after addition of 0.4, 0.8, 1.2, 1.6, 2.0, 2.4, 3.2, and 4.0 equiv of NADH.

Dihydrolipoamide dehydrogenases, like many flavoenzymes, can oxidize NADH by reducing molecular oxygen to hydrogen peroxide. This intrinsic NADH oxidase activity is usually much slower than the dihydrolipoamide dehydrogenase activity. Assaying across the yellow fractions of the Q-Sepharose FF and Phenyl Sepharose HP columns showed a 5-fold enhancement in the rate of oxidation of NADH upon addition of 0.5 mM D,L-lipoamide (see also Table 2). This activity precisely coeluted with the 50 kDa band and the intensity of the yellow color in the fractions. These results demonstrate that the *lpdC* gene of *M. tuberculosis* codes for dihydrolipoamide dehydrogenase.

Spectral Characterization. The visible absorption spectrum of oxidized dihydrolipoamide dehydrogenase (uppermost spectrum, Figure 2) shows the presence of a flavin cofactor as observed for dihydrolipoamide dehydrogenases from other organisms and other members of the pyridine nucleotide: disulfide oxidoreductase family (*1*). There are absorbance maxima at 375 and 458 nm with a shoulder at ~485 nm and minima at 308 and 403 nm. Figure 2 also shows the change in the absorption spectrum of *M. tuberculosis* dihydrolipoamide dehydrogenase as NADH is titrated anaerobically at pH 7.5 and 25 °C. The absorbance maximum at 458 nm decreases and is blue-shifted. The absorbance increases at longer wavelengths extending to >700 nm with a clear isosbestic point at ~507 nm.

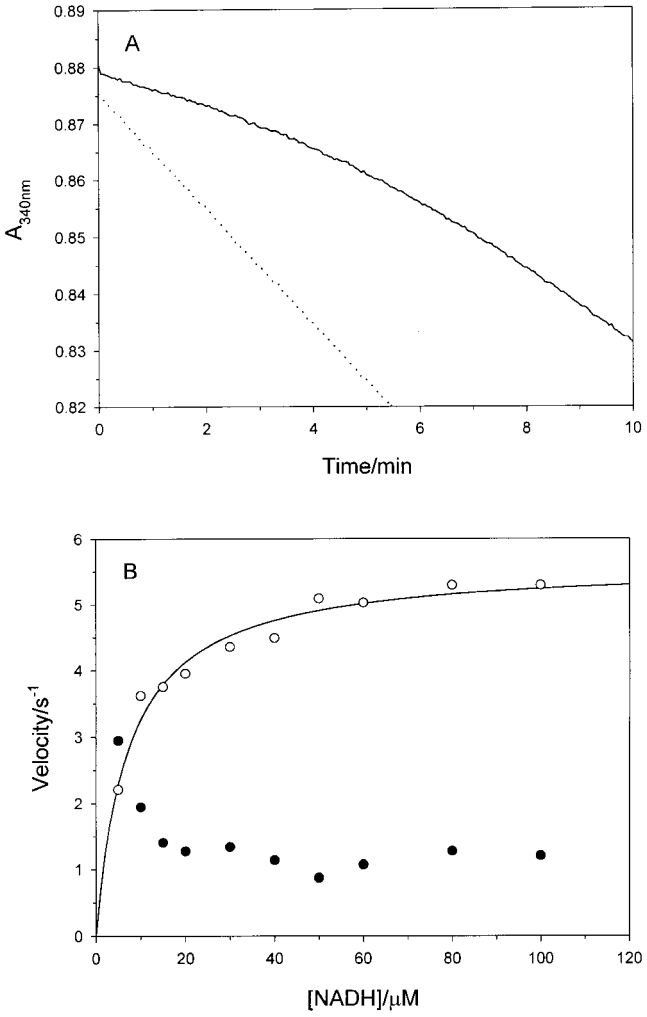

FIGURE 3: NAD^+ relieves the inhibition of *M. tuberculosis* dihydrolipoamide dehydrogenase by NADH. (A) Typical time course illustrating an increase in the activity of *M. tuberculosis* dihydrolipoamide dehydrogenase as a product (NAD^+) of the enzymatic reaction accumulates (solid line). Inclusion of 20 μM NAD^+ in the assay linearizes the time course and increases the initial rate 5-fold (dotted line). Assays contained: 100 mM Hepes, pH 7.5, 1 mM EDTA, 5% (v/v) methanol, 100 μM NADH, 2.5 mM D,L-lipoamide, 5 nM *M. tuberculosis* dihydrolipoamide dehydrogenase, with (dotted line) and without (solid line) 20 μM NAD^+. Assays were initiated by the addition of enzyme. (B) NADH titration of *M. tuberculosis* dihydrolipoamide dehydrogenase illustrating substrate NADH inhibition (closed circles, no added NAD^+) and relief of inhibition by 40 μM NAD^+ (open circles) The solid line is a fit of the data to eq 2 with $k_{cat}^{app} = 5.6 \pm 0.2\ s^{-1}$ and K_m^{app} (NADH) $= 7.3 \pm 0.9$ μM. Assay conditions were identical to those of panel A.

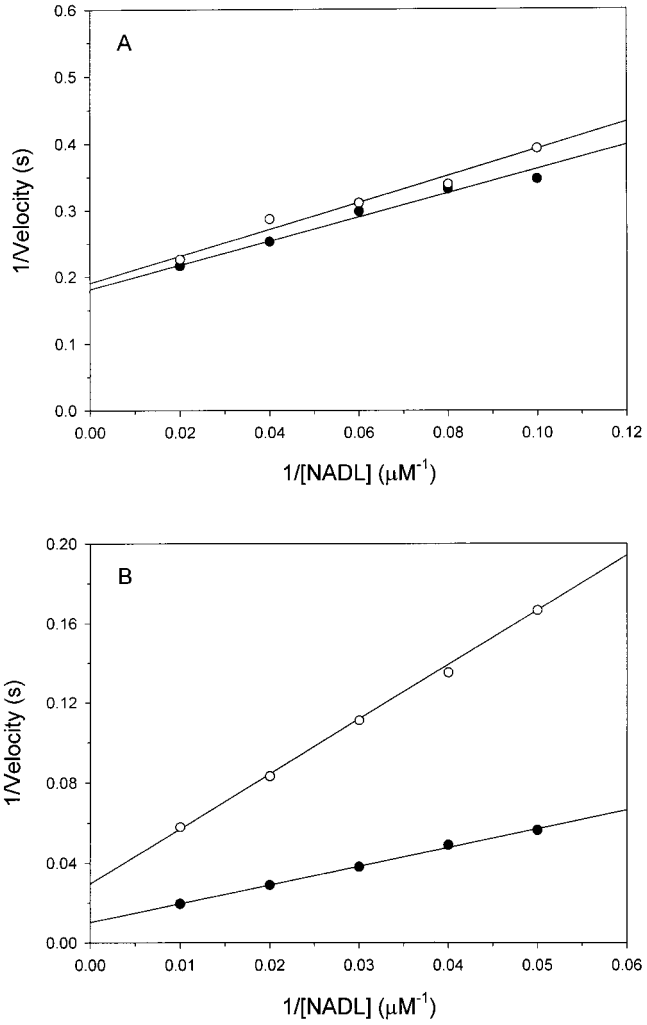

FIGURE 4: Primary deuterium kinetic isotope effects arising from deuterium substitution at the C_4-*proS* position of NADH, illustrating that hydride transfer to FAD is not rate limiting when D,L-lipoamide is the oxidant (panel A) versus rate-limiting hydride transfer when 5-HNQ is the oxidant (panel B). Assays contained (A) 100 mM Hepes, pH 7.5, 1 mM EDTA, 5% (v/v) methanol, 2.5 mM D,L-lipoamide, 2 nM *M. tuberculosis* dihydrolipoamide dehydrogenase, 40 μM NAD^+, and 10−50 μM NADH (closed circles) or 10−50 μM [*4S*-^{2}H]-NADH (open circles), and (B) 100 mM Hepes, pH 7.5, 1 mM EDTA, 1% (v/v) acetonitrile, 0.5 mM 5-HNQ, 0.5 nM *M. tuberculosis* dihydrolipoamide dehydrogenase, and 20−100 μM NADH (closed circles) or 20−100 μM [*4S*-^{2}H]-NADH (open circles). The solid lines are fits to eq 4 (panel A) and eq 5 (panel B). L = H or D in NADL.

NAD^+ Relieves the Inhibition Caused by NADH. Figure 3A shows a typical time course for dihydrolipoamide dehydrogenase using NADH and D,L-lipoamide as the substrate pair. The activity of dihydrolipoamide dehydrogenase increases with time as a product of the enzymatic reaction accumulates (solid line). Inclusion of 20 μM NAD^+ in the assay linearizes the time course (dotted line) concomitant with a 5-fold increase in the initial rate.

Figure 3B shows the dependence of the initial velocity on the concentration of NADH at 2.5 mM D,L-lipoamide in the absence (closed circles) and presence (open circles) of 40 μM NAD^+. In the absence of NAD^+, NADH strongly inhibits the enzyme resulting in a nonhyperbolic plot. The presence of 40 μM NAD^+ relieves the inhibition caused by NADH resulting in a hyperbolic plot with an apparent K_m for NADH of 7.3 μM. The kinetic parameters (Tables 1 and 2) and the primary deuterium kinetic isotope effects (Table 3) for the NADH and D,L-lipoamide pair were performed in the presence of 40 μM NAD^+, a concentration affording maximal activation (data not shown). NAD^+ begins to inhibit at concentrations of >80 μM. This behavior is specific for NADH since all alternate reduced pyridine nucleotide substrates used (Table 1) are free of such effects, and thus, no NAD^+ was included in these assays. Linear time courses were also observed when quinones or $tNAD^+$ were used as oxidants in reactions containing NADH, and NAD^+ was also omitted from these assays.

Steady-State Kinetics. Initial velocity data from assays in which the concentration of any of the reduced pyridine

Table 1: Steady-State Kinetic Constants for Reaction of Reduced Pyridine Nucleotide Analogs with D,L-Lipoamide Catalyzed by *M. tuberculosis* Dihydrolipoamide Dehydrogenase[a]

reductant	k_{cat} (s^{-1})	K_m [Lip(S)$_2$] (mM)	K_m (reductant) (μM)	k_{cat}/K_m [Lip(S)$_2$] ($M^{-1}s^{-1}$)	k_{cat}/K_m (reductant) ($M^{-1}s^{-1}$)
NADH[b]	36 ± 7[c,d]	16 ± 3[c]	7.3 ± 0.9[d]	$(2.3 \pm 0.6) \times 10^3$[c]	$(4.9 \pm 1.1) \times 10^6$
tNADH	14 ± 1	5.8 ± 0.6	110 ± 10	$(2.4 \pm 0.3) \times 10^3$	$(1.3 \pm 0.2) \times 10^5$
NHDH	16 ± 4	6.4 ± 1.8	2600 ± 700	$(2.5 \pm 0.9) \times 10^3$	$(6.2 \pm 2.2) \times 10^3$
APADH	1.6 ± 0.1	0.56 ± 0.03	390 ± 20	$(2.9 \pm 0.2) \times 10^3$	$(4.1 \pm 0.3) \times 10^3$

[a] At pH 7.5, 25 °C. The values of the kinetic constants were obtained from fits of the data of five different concentrations of the reductant at five fixed levels of the oxidant to eq 3, except where stated. [b] Reactions contained 40 μM NAD^+ (see Results). [c] At saturating (100 μM) NADH. [d] At 2.5 mM D,L-lipoamide; since D,L-lipoamide is not saturating, the K_m (NADH) and k_{cat} values are underdetermined.

Table 2: Steady-State Kinetic Constants for Reaction of NADH with Several Oxidants Catalyzed by *M. tuberculosis* Dihydrolipoamide Dehydrogenase[a]

oxidant	k_{cat} (s^{-1})	K_m (oxidant)	K_m (NADH) (μM)	k_{cat}/K_m (oxidant) ($M^{-1}s^{-1}$)	k_{cat}/K_m (NADH) ($M^{-1}s^{-1}$)
D,L-lipoamide[b]	36 ± 7[c,d]	16 ± 3 mM[c]	7.3 ± 0.9[d]	$(2.3 \pm 0.6) \times 10^3$[c]	$(4.9 \pm 1.1) \times 10^6$
D,L-lipoate[c]	2.6 ± 0.5	120 ± 25 mM	−[c]	$(2.2 \pm 0.6) \times 10^1$	−[c]
$tNAD^+$	17 ± 1	36 ± 3 μM	4.1 ± 0.3	$(4.7 \pm 0.5) \times 10^5$	$(4.2 \pm 0.4) \times 10^6$
O_2[e]	0.25 ± 0.01	−[e]	8.4 ± 2.3	−[e]	$(3.0 \pm 0.8) \times 10^4$
5-HNQ	165 ± 10	0.29 ± 0.02 mM	161 ± 10	$(5.7 \pm 0.5) \times 10^5$	$(1.0 \pm 0.1) \times 10^6$
DMBQ	190 ± 10	0.86 ± 0.06 mM	156 ± 10	$(2.2 \pm 0.2) \times 10^5$	$(1.2 \pm 0.1) \times 10^6$

[a] At pH 7.5, 25 °C. The values of the kinetic constants were obtained from fits of the data of five different concentrations of NADH at five fixed levels of the oxidant to eq 3, except where stated. [b] Reactions contained 40 μM NAD^+ (see Results). [c] At 100 μM NADH. [d] At 2.5 mM D,L-lipoamide; since D,L-lipoamide is not saturating, the above K_m (NADH) and k_{cat} values are underdetermined. [e] At ambient O_2 levels (230 μM).

Table 3: Primary Deuterium Kinetic Isotope Effects for *M. tuberculosis* Dihydrolipoamide Dehydrogenase Using [*4S*-^{2}H]-NADH as the Deuterated Substrate[a]

oxidant	$^D(V/K)_{NADH}$	$^DV_{app}$[d]
D,L-lipoamide[b]	1.12 ± 0.15	1.05 ± 0.07
5-HNQ[c]	2.95 ± 0.03	2.95 ± 0.03

[a] Data were obtained in 100 mM HEPES, pH 7.5, at 25 °C. [b] At 2.5 mM D,L-lipoamide in the presence of 40 μM NAD^+ (see Results). [c] At 0.5 mM 5-HNQ. [d] These are not true ^DV effects because the oxidant was at subsaturating levels.

Table 4: Solvent Isotope Effects for *M. tuberculosis* Dihydrolipoamide Dehydrogenase[a]

oxidant	$^{D_2O}(V/K)_{APADH}$	$^{D_2O}(V/K)_{RSSR}$	$^{D_2O}V_{app}$[f]	k_{cat}/K_m ($M^{-1}s^{-1}$)
D,L-lipoamide	0.73 ± 0.03[b]	0.77 ± 0.03[c]	0.77 ± 0.01	$12\,000 \pm 400$
DTP	0.75 ± 0.06[d]	0.71 ± 0.02[e]	0.56 ± 0.15	86 ± 22

[a] Data were obtained in 100 mM MES pH(D) 5.8, at 25 °C. [b] At 0.5 mM D,L-lipoamide. [c] At 100 μM APADH. [d] At 2.5 mM DTP. [e] At 25 μM APADH. [f] These are not true ^{D_2O}V effects because the cosubstrate was at subsaturating levels.

nucleotide analogs was varied at various fixed levels of the cosubstrate D,L-lipoamide showed a pattern of parallel lines in double-reciprocal plots (data not shown). Parallel reciprocal plots were also observed with NADH as the reductant and 5-HNQ, DMBQ, or $tNAD^+$ as oxidants. Data were fitted to eq 3 and the kinetic parameters are tabulated in Tables 1 and 2.

The very high K_m for D,L-lipoamide (16 mM) and its moderate solubility (concentrations were limited to ≤2.5 mM) hampered the accurate determination of the kinetic parameters when NADH was the reductant. We thus elected to determine the kinetic parameters for this substrate pair by titrating one substrate at a single saturating (or as high as attainable) concentration of the cosubstrate. We note that the K_m(NADH) and k_{cat} in Tables 1 and 2 for this substrate pair are both underdetermined.

Primary Deuterium Kinetic Isotope Effects. To determine the stereospecificity of hydride transfer from NADH (*proR* versus *proS*) to FAD on the enzyme, and to probe whether hydride transfer is rate determining, we measured primary deuterium kinetic isotope effects arising from deuterium substitution at the C_4-*proS* position in the nicotinamide ring of NADH with D,L-lipoamide and 5-HNQ as oxidants. Reciprocal plots of these experiments are shown in Figure 4, and the results are shown in Table 3.

Solvent Isotope Effects. The presence of several proton-transfer steps in the reaction, any of which might be rate limiting, led us to carry out solvent isotope effects. Given the nonlinear time courses exhibited by NADH and the potential of a solvent isotope effect on the activation by NAD^+ (thus complicating interpretation), we elected to use APADH as the reductant, which gives linear time courses with both D,L-lipoamide and DTP (below) as oxidants. Using 100 μM APADH, both V and $V/K_{Lip(S)_2}$ decrease at high pH with apparent pK_a values of 7.3 ± 0.1 and 7.0 ± 0.1, respectively (data not shown). The solvent isotope effects were thus performed at pH(D) = 5.8, a pH region where both V and $V/K_{Lip(S)_2}$ are insensitive to changes in the pH. In addition to D,L-lipoamide, we also used DTP as a control. The product of DTP reduction is 4-thiopyridone; the pK_a of the thiol group of 4-thiopyridone is 1.43 (*10*) and, hence, does not require protonation at pH 5.8 (see Discussion). The solvent isotope effects are tabulated in Table 4.

DISCUSSION

Problem of Functional Assignment. Approximately 40% of the *orfs* identified in the sequencing of genomes of microorganisms have unknown function (*11*). Some of the *orfs* that have been assigned function by homology alone may be incorrectly assigned (*11*). This problem is exemplified by the five *orfs* we identified in *M. tuberculosis* that

bear significant amino acid sequence identity to dihydrolipoamide dehydrogenases. Two of the *orfs* (*lpdA* and *lpdB*) have been designated as probable dihydrolipoamide dehydrogenases based solely on homology to these enzymes (*6*). We have shown that purified *lpdA* does not have dihydrolipoamide dehydrogenase activity (A.A. and J.S.B., unpublished results). This was perhaps not surprising since this protein lacks both Cys^N and the His-Glu pair proposed to function as a general acid (Figure 1). Likewise, *lpdB* is unlikely to exhibit dihydrolipoamide dehydrogenase activity since it lacks this His residue. On the other hand, *lpdC* contains the complete set of catalytic residues essential for dihydrolipoamide dehydrogenase activity, and the expressed purified protein can reduce D,L-lipoamide in an NADH-dependent manner. Further, *lpdC* displays all the properties expected for previously characterized dihydrolipoamide dehydrogenases: homodimeric flavoprotein, ping−pong kinetics (below), charge-transfer absorbance at 530 nm, inhibition by NADH and relief of inhibition by NAD^+ (*1*). Thus, high sequence homology alone is not enough to assign function. Knowledge of key catalytic residues and cofactor binding motifs previously derived from thorough enzymological and structural studies of homologs,[2] orthologs, and paralogs, however, appears to significantly increase the successful assignment of function.

Mechanism by Which NAD^+ Relieves the Inhibition Caused by NADH. The active form of dihydrolipoamide dehydrogenase that catalyzes the oxidative half-reaction has been proposed to be the two-electron reduced enzyme (EH_2) where the redox-active disulfide is reduced and the FAD is oxidized (*12*). Dihydrolipoamide dehydrogenase can accommodate another two electrons where the flavin cofactor is also reduced ($FADH_2$). This four-electron reduced enzyme (EH_4) is thought to be inactive (*12*) and can accumulate at high concentrations of NADH. The *E. coli* enzyme is more susceptible to inhibition by NADH than the pig heart enzyme because the redox-potential for the E/EH_2 (−264 mV) and EH_2/EH_4 (−317 mV) couples (*13*) are more positive than the corresponding values for the pig heart enzyme (−280 and −346 mV, respectively) (*14*). By this criterion, the *M. tuberculosis* enzyme is more similar to the *E. coli* enzyme than the pig heart enzyme since NADH is inhibitory at concentrations ≥5 μM and this inhibition can be partially relieved by added NAD^+ (Figure 3). It has been proposed that the added NAD^+ raises the steady-state levels of the active (EH_2) relative to the inactive (EH_4) form of the enzyme (*12*).

Reaction Intermediates of Dihydrolipoamide Dehydrogenase. The change in the visible absorption spectrum upon anaerobic addition of reduced pyridine nucleotides has been used to detect reaction intermediates for many flavoenzymes. As shown in Figure 2, anaerobic addition of NADH to dihydrolipoamide dehydrogenase results in an increase in absorbance at ∼530 nm. This spectroscopic signal is a hallmark of the charge-transfer complex between the thiolate of Cys^C and oxidized FAD (EH_2), a proposed intermediate in the reaction of the flavoprotein pyridine nucleotide: disulfide oxidoreductases (*1*). For the *M. tuberculosis* enzyme, the increase of the long-wavelength absorbance extends to >700 nm, indicating also the presence of an $FADH^-/NAD^+$ charge-transfer species (*15*, *16*) which has also been proposed to be an intermediate in the reaction.

Steady-State Kinetics. The pattern of parallel lines observed on double-reciprocal plots when any of the reduced pyridine nucleotide analogs were varied at various fixed levels of D,L-lipoamide is consistent with a ping−pong mechanism. A distinguishing feature of this mechanism is the absence of the ternary complexes $Lip(S)_2 \cdot E_{OX} \cdot NADH$ and $Lip(SH)_2 \cdot E_{OX} \cdot NAD^+$. Thus, if the mechanism is ping−pong, dihydrolipoamide dehydrogenase should catalyze the interconversion of NADH and NAD^+ (or any of its analogs) in the absence of D,L-lipoamide or D,L-dihydrolipoamide. Incubation of dihydrolipoamide dehydrogenase with NADH and $tNAD^+$, but in the absence of D,L-lipoamide or D,L-dihydrolipoamide, resulted in the formation of tNADH and NAD^+ at a rate ($k_{cat} = 17\ s^{-1}$, Table 2) that was comparable with that of the tNADH and D,L-lipoamide pair ($k_{cat} = 14\ s^{-1}$, Table 1). This experiment provides strong evidence that the kinetic mechanism is ping−pong. Finally, ping−pong mechanisms have been proposed for all dihydrolipoamide dehydrogenases studied thus far (*1*).

Table 1 lists the kinetic parameters for reaction of NADH and several reduced pyridine nucleotide analogs with D,L-lipoamide. While the k_{cat}/K_m values for D,L-lipoamide are similar ($2.3-2.9 \times 10^3\ M^{-1}s^{-1}$) regardless of the nature of the reductant, as required for a ping−pong mechanism, those for NADH and analogs vary by 3 orders of magnitude. NADH, as expected, is the best substrate as evaluated by the k_{cat}/K_m value. Though the slower rates for tNADH and APADH might be partly explained by the more positive redox potentials (−285 and −258 mV, respectively) for these analogs relative to NADH (−320 mV), the redox potential for NHDH is identical to that of NADH. The higher K_m for NHDH is thus most likely due to weaker steady-state affinity for the enzyme resulting in a k_{cat}/K_m value that is 3 orders of magnitude lower than NADH.

The natural substrate for dihydrolipoamide dehydrogenase is lipoic acid covalently bonded via an amide linkage to the ϵ-amino group of a lysine residue in the E2 subunit of the pyruvate and α-ketoglutarate dehydrogenase multienzyme complexes (*2*). Given the difficulty associated with preparing substrate amounts of the E2 enzyme for steady-state kinetic studies, two commercially available truncated versions (D,L-lipoamide and D,L-lipoate) of the natural substrate have been used previously in assays for dihydrolipoamide dehydrogenase. The high K_m values for D,L-lipoamide (16 mM) and D,L-lipoate (120 mM, Table 2) reflect both the nonphysiological nature of these substrates and the physiological and physical association of the lipoylated E2 with the dehydrogenase.

Perhaps the most surprising result is the efficiency with which quinones are reduced by dihydrolipoamide dehydrogenase (Table 2). The k_{cat} values are 4−6-fold higher than D,L-lipoamide reduction, and the k_{cat}/K_m values of $2.2-5.7 \times 10^5\ M^{-1}\ s^{-1}$ are 2 orders of magnitude higher than for D,L-lipoamide. Though the ability of dihydrolipoamide dehydrogenases to catalyze diaphorase reactions has been known for some time (*17*), rates as high as these have not been reported. The pig heart enzyme catalyzes the reduction

[2] Homologs are proteins derived from a common ancestor. Orthologs are homologs in different species that catalyze the same reaction. Paralogs are homologs in the same species that catalyze different reactions.

Scheme 1: Proposed Chemical Mechanism for *M. tuberculosis* Dihydrolipoamide Dehydrogenase

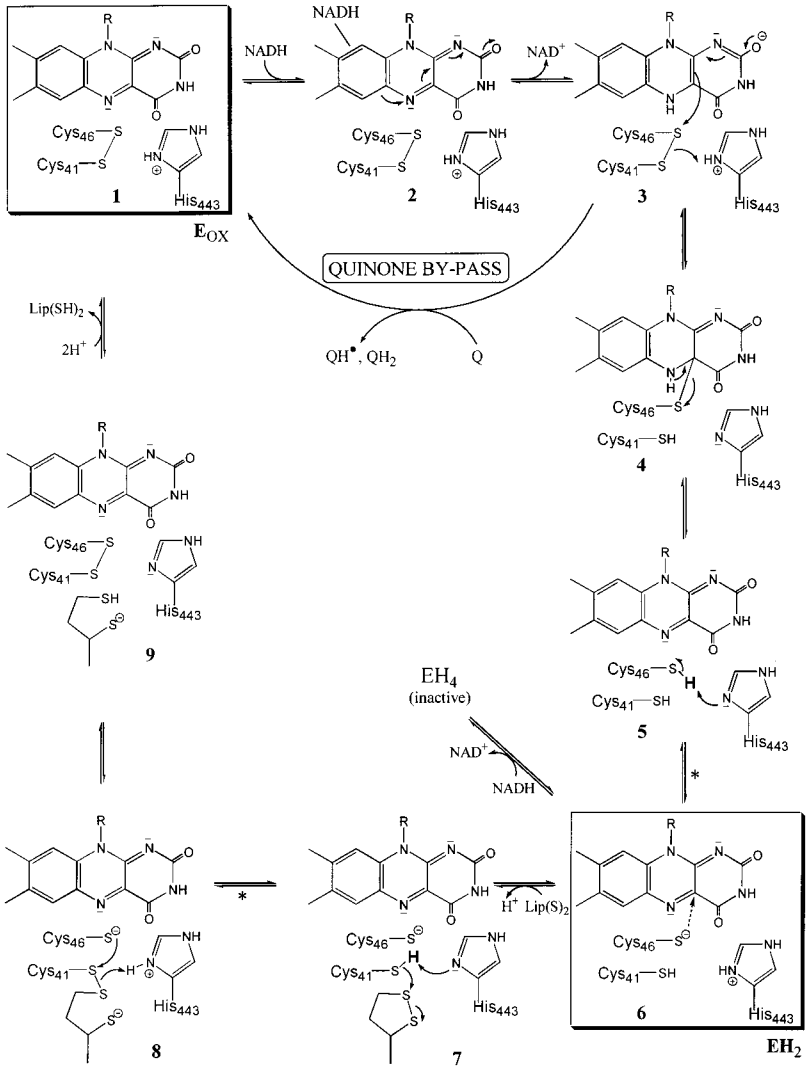

of quinones at rates only 10% that of lipoamide reduction (*18*). The *Mycobacterium smegmatis* enzyme catalyzes reduction of quinones at rates that are moderately faster (2-fold) than lipoamide reduction (*19*). Whether reduction of quinones, for example membrane-bound ubiquinones, by mycobacterial dihydrolipoamide dehydrogenases occurs in vivo, and whether this is physiologically significant is unknown at this time.

Primary Deuterium Kinetic Isotope Effects. The catalytic cycle of dihydrolipoamide dehydrogenase has been determined in significant detail (Scheme 1). NADH binds to the oxidized enzyme (E_{OX}) and reduces the tightly bound FAD. Internal electron transfer to the redox-active disulfide then generates the anaerobically stable two-electron reduced form of the enzyme (EH_2) which is observed spectroscopically (Figure 2). Cys^N (Cys_{41} in the *M. tuberculosis* protein) is now thought to be protonated while Cys^C (Cys_{46} in the *M. tuberculosis* protein) exists as the free thiolate (*14*). Interaction of the free thiolate of Cys^C with FAD is thought to be responsible for the charge-transfer complex observed at wavelengths >507 nm (Figure 2). Departure of NAD^+ completes the reductive half-reaction. In the oxidative half-reaction, the substrate lipoamide binds to the enzyme, and Cys^N forms a mixed disulfide with the substrate. The free thiolate of Cys^C then attacks the mixed disulfide to form dihydrolipoamide and to regenerate E_{OX}. This reaction is general-acid catalyzed by the essential and conserved His-Glu pair located near the C-terminus of the enzyme (His_{443}-Glu_{448} in the *M. tuberculosis* sequence). Release of dihydrolipoamide completes the oxidative half-reaction for another round of catalysis.

To probe the nature of the rate-limiting steps in the catalytic cycle of dihydrolipoamide dehydrogenase from *M. tuberculosis*, we measured primary deuterium and solvent kinetic isotope effects. To determine whether hydride transfer from NADH to FAD is rate limiting, we measured primary deuterium kinetic isotope effects arising from deuterium substitution at the C_4-*proS* position of the nicotinamide ring of NADH. With D,L-lipoamide as oxidant, the isotope effects on V_{app} and V/K_{NADH} are small (Figure 4 and Table 3) suggesting that hydride transfer is not rate limiting when D,L-lipoamide is the oxidant. The rate-limiting step must occur after hydride transfer for reasons discussed below.[3]

The diaphorase activity (the NADH-dependent reduction of alternate electron acceptors such as $K_3Fe(CN)_6$, DCPIP,

[3] Depression of isotope effects from intrinsic $^DV/K_{NADH}$ values may also arise if NADH is sticky, that is, hydride transfer from NADH to FAD occurs faster than NADH dissociates from the NADH·E_{ox} complex. However, this is unlikely because a large isotope effect on $^DV/K_{NADH}$ was observed using 5-HNQ as oxidant (Table 3).

quinones, and O_2) of dihydrolipoamide dehydrogenases does not require an intact redox-active disulfide. Individual point mutants of the *E. coli* dihydrolipoamide dehydrogenase (C44S and C49S) (*20*), and the pig heart enzyme monoalkylated (EHR) at Cys^N (*21*) are essentially devoid of dihydrolipoamide dehydrogenase activity, but the diaphorase activity is unaffected. Reduction of quinones then, is thought to occur by one electron transfer from the reduced FAD to the quinone acceptor. All steps occurring after hydride transfer in the normal catalytic cycle would then be by-passed by quinones (Scheme 1), and would allow for expression of the primary deuterium kinetic isotope effect if hydride transfer is rate limiting in these reactions. With 5-HNQ as oxidant, the isotope effects on V and V/K_{NADH} are now large and equivalent (Figure 4 and Table 3). We conclude that (1) with 5-HNQ as oxidant, hydride transfer is rate limiting and that the measured isotope effects are intrinsic because the isotope effects on V and V/K are equal, (2) D,L-lipoamide reduction involves additional step(s) that are effectively by-passed by quinones, and (3) these additional step(s) are significantly slower than reduction of the FAD by NADH resulting in the depression of the isotope effect on V/K_{NADH} from 2.95 (5-HNQ as oxidant) to 1.12 (D,L-lipoamide as oxidant). The presence of isotope effects also establishes that hydride transfer from NADH is *proS*-specific, as has been demonstrated for all enzymes in the pyridine nucleotide: disulfide oxidoreductase family (*1*).

Somewhat different results have been reported for the pig heart enzyme (*18*). The primary kinetic isotope effects observed using quinones as oxidants were similar to our results, with equivalent V and V/K effects observed ($^DV \approx {}^DV/K = 1.9-3.0$). Though no isotope effect was observed on V with lipoamide as oxidant, a V/K effect of $\sim$2 argues that hydride transfer is at least partially rate limiting for the reductive half-reaction in the pig heart enzyme. For the *M. tuberculosis* enzyme, we think that formation of the Cys_{46}−FAD charge-transfer complex, a step that occurs after hydride transfer, limits the reductive half-reaction for reasons that will be discussed in the next section.

Solvent Isotope Effects. Having established that the rate-limiting step(s) in lipoamide reduction must come after hydride transfer, we focused our efforts on proton-transfer steps that occur later in the catalytic cycle using solvent kinetic isotope effects. Though, as shown in Scheme 1, many proton-transfer steps occur between substrates, enzymic thiolates/thiols, and His_{443} in the catalytic cycle of dihydrolipoamide dehydrogenase, only some may be of kinetic importance. Our analysis relies on, and is simplified by, the unique fractionation factors of protonated mercaptans (*22*). With their strong preference for protons over deuterons ($\phi = 0.4-0.6$), any rate-limiting proton transfer from a thiol will lead to an inverse solvent kinetic isotope effect. Inverse solvent kinetic isotope effects were observed on V/K whether D,L-lipoamide or APADH is the variable substrate (Table 4). The proton inventory was linear, indicative of a single proton being transferred in the solvent sensitive step. This suggests that (1) both the reductive, as reflected in V/K_{APADH}, and oxidative, as reflected in $V/K_{Lip(S)_2}$, half-reactions involve an at least partially rate-limiting proton-transfer step, and (2) deprotonation of a thiol is responsible for the inverse effect. Problems with substrate solubility and/or high substrate K_m values precluded analysis of the solvent isotope effects at saturating levels of the cosubstrate. Thus, no conclusions can be made regarding rate-limiting steps for the overall reaction because ^{D_2O}V measurements were not possible.

To determine whether the thiol whose fractionation factor yields the inverse solvent kinetic isotope effect is localized on the enzyme or on the substrate lipoamide, we measured solvent kinetic isotope effects using DTP as an alternate dithiol substrate. The product of DTP reduction is 4-thiopyridone, whose formation requires no general-acid catalysis since the pK_a value of the thiol moiety is 1.43 (*10*). Inverse solvent kinetic isotope effects of similar magnitude to D,L-lipoamide were also observed on V/K whether DTP or APADH is varied (Table 4). The proton inventory was also linear indicative of a single proton being transferred in the solvent sensitive step. This result localizes the solvent-sensitive proton transfer to the thiol on the enzyme.[4] We propose that deprotonation of Cys_{46} in the reductive half-reaction, and deprotonation of Cys_{41} in the oxidative half-reaction gives rise to the observed inverse solvent kinetic isotope effects (Scheme 1).[5]

This laboratory has previously measured solvent kinetic isotope effects on the pig heart dihydrolipoamide dehydrogenase (*25*), glutathione reductases from three species (*26*), *M. tuberculosis* mycothione reductase (*27*), and *Trypanosoma congolense* trypanothione reductase (*28*). In all of these studies, *normal* solvent kinetic isotope effects were observed in the direction of disulfide reduction (eq 1). For the pig heart dihydrolipoamide dehydrogenase, inverse solvent isotope effects were only observed in the reverse direction. These differences may be explained in either of two ways.

(1) We conducted the solvent isotope effects at pH(D) = 5.8, which is significantly lower than all other prior studies, which were performed between pH(D) = 7.0 and 8.1. The extent to which inverse solvent isotope effects will be observed depends on the protonation state of the thiol responsible for the inverse effect. It is possible that, at pH(D) = 5.8, Cys^C is protonated in EH_2 (Scheme 1), thus giving rise to inverse solvent isotope effects in the reductive half-reaction (this study), while at pH(D) > 7.0, Cys^C in the other enzymes is largely deprotonated and inverse solvent isotope effects are not observed. Supporting this notion is the disappearance of the Cys^C-FAD charge-transfer complex in the two-electron reduced form of the pig heart dihydrolipoamide dehydrogenase below a single pK_a of 5.0 (*14*). A

[4] The pK_a values for the pyridinium nitrogen atoms in the substrate, DTP, are expected to be similar to the value of 5.14 for the nitrogen atom in pyridine (*10*). The pK_a value for the nitrogen atom in the product, 4-thiopyridone, is 8.86 (*10*) and proton transfer to this nitrogen atom is required as product forms at the experimental pH of 5.8. However, such a proton transfer, if at all rate limiting, is not expected to give rise to an inverse solvent kinetic isotope effect because the fractionation factors for secondary amines are in the range 1.01−1.49 (*22*).

[5] An alternative explanation for the inverse solvent isotope effects is the formation of a low-barrier hydrogen bond (LBHB) between His_{443} and Glu_{448} during enzymic-disulfide reduction as Cys_{41} becomes protonated. The distance between the His_{467}-ND1 and Glu_{472}-OE2 atoms of 2.77 Å in the high-resolution structure of human glutathione reductase (oxidized form) indicates the presence of a strong hydrogen bond with the potential of getting shorter, and hence, stronger during enzymic-disulfide reduction (*23*). This is similar to the LBHB observed in the His-Glu diad of the serine proteases (*24*). The presence or absence of such a LBHB in *M. tuberculosis* dihydrolipoamide dehydrogenase is currently under investigation.

similar argument may be made for the protonation state of Cys^N, which we think is responsible for the inverse solvent isotope effect observed in the oxidative half-reaction. It is thought that the two-electron reduced enzyme in dihydrolipoamide dehydrogenase is doubly protonated (EH_2) (*14*) whereas in glutathione reductase it is a mixture of mono- (EH^-) and doubly (EH_2) protonated species (*29*), the difference perhaps being the pK_a of Cys^N in the different homologs and orthologs.

(2) Inverse solvent isotope effects will be observed if proton transfer from the thiol is at least partially rate limiting. It is possible that there are differences in the rate-limiting steps among the different homologs, orthologs, and paralogs. Previous rapid kinetic stopped-flow work on the pig heart dihydrolipoamide dehydrogenase have established that the oxidative half-reaction is rate limiting (*30, 31*). In addition, this laboratory has recently carried out stopped-flow studies (*27*) on the *M. tuberculosis* mycothione reductase and have established that the rates of the oxidative and reductive half-reactions are similar. Similar rates for the two half-reactions have also been measured for yeast glutathione reductase (*1*).

The differences in the solvent kinetic isotope effects and the primary deuterium kinetic isotope effects between the *M. tuberculosis* and pig heart dihydrolipoamide dehydrogenases suggest that the rate-limiting steps for these two orthologs are different. In addition, the turnover number of the *M. tuberculosis* enzyme is slower than the pig heart enzyme. The fastest rates (k_{cat}) that we have measured are 160−190 s^{-1} with quinones as oxidants (Table 2). The fact that large and probably intrinsic primary kinetic isotope effects are seen in the steady-state using quinones as oxidants suggests that the reductive half-reaction cannot be significantly faster than these rates. The value of 160−190 s^{-1} is well below the lower limit of 800 s^{-1} (*30*) that was measured for the reductive half-reaction by stopped-flow with the pig heart enzyme under similar conditions. We are in the process of conducting rapid kinetic stopped-flow experiments on the *M. tuberculosis* dihydrolipoamide dehydrogenase to directly measure the rates of the oxidative and reductive half-reactions. The fact that the *M. tuberculosis* enzyme is relatively slow may also allow the detection of a transient, reduced flavin ($E{\cdot}FADH^-$), an intermediate that we propose exists (Scheme 1), but has not as yet been observed for any wild-type dihydrolipoamide dehydrogenase, probably because its formation and breakdown rates are too rapid to measure even with stopped-flow methods.

Chemical Mechanism for M. tuberculosis Dihydrolipoamide Dehydrogenase. We present a chemical mechanism (Scheme 1) for the *M. tuberculosis* enzyme similar to the one proposed earlier for the pig heart enzyme (*25*) modified slightly to accommodate our findings. NADH binds to E_{OX} and delivers a hydride from the C_4-*proS* position of the pyridine ring to the FAD. The resulting reduced flavin intermediate (**3**) is unstable and has not as yet been observed spectrophotometrically for any wild-type enzyme. For reasons discussed above, this is most likely the site of quinone electron-transfer reactions. Disulfide reduction then occurs to generate a covalent Cys_{46}−C4a flavin adduct (**4**) (*32*) assisted by protonation of Cys_{41} by the protonated imidazole of His_{443}. Collapse of the Cys_{46}−C4a adduct generates one of the prototautomers of EH_2 (**5**). Deprotonation of Cys_{46} by the neutral imidazole of His_{443} generates the other prototautomer of EH_2 (**6**), which is responsible for the charge-transfer complex observed at ∼530 nm. We think that this proton-transfer step, marked with an astersik (∗), limits and results in the observed inverse solvent isotope effect.[5] Our proposal that the rate-limiting step in the reductive half-reaction occurs after hydride transfer is also supported from stopped-flow studies of an H450S point mutant of the *Azotobacter vinelandii* dihydrolipoamide dehydrogenase, where reduction of the FAD by NADH occurs rapidly whereas subsequent reduction of the enzymic disulfide is slower relative to wild-type (*15*). The result is the dramatic stabilization of the $FADH^-/NAD^+$ charge-transfer complex by a factor of 1000. Similar results were obtained with the *E. coli* glutathione reductase H439A mutant (*16*).

In the oxidative half-reaction, lipoamide binds to the enzyme to form **7**. Though we have no evidence for concomitant loss of a proton from His_{443} to solution, we chose to draw it as such to reduce the number of subsequent proton-transfer steps involved, thereby simplifying the mechanism. For a more detailed mechanism, the reader is referred to Leichus and Blanchard (*25*). Deprotonation of Cys_{41} by His_{443} increases its nucleophilicity toward lipoamide. We propose that this proton-transfer step, also marked with an asterisk (∗), limits and leads to the inverse solvent kinetic isotope effect observed in the oxidative half-reaction. The result is the formation of a mixed disulfide between Cys_{41} and lipoamide (**8**). Next, Cys_{46} attacks the mixed Cys_{41}-substrate disulfide. This reaction is general-acid catalyzed by the protonated imidazole of His_{443}. However, we do not think that this step is rate limiting because inverse solvent kinetic isotope effects were still observed with DTP as substrate, reduction of which requires no general-acid catalysis (above). The result is reduced lipoamide and regeneration of the Cys_{41}−Cys_{46} enzymic disulfide (**9**). Release of product completes the cycle.

As discussed above, the result of losing a proton to solution in going from **6** to **7** in step 6, reduced the number of subsequent proton-transfer steps and intermediates in the chemical mechanism. Another consequence is that the enzyme-bound product of the reaction is *mono*protonated reduced lipoamide. The pK_a values of the two thiols of dihydrolipoamide are >9.5 in solution (*33*), and monoprotonated reduced lipoamide is, therefore, not favored at neutral pH. However, its existence on the enzyme cannot be ruled out if it is stabilized, for example, by the equal sharing of the proton between the C_6 and C_8 sulfur atoms of reduced lipoamide. We note that there is no evidence that it is the C_8 sulfur of lipoamide that participates in mixed disulfide bond formation in the catalytic cycle; we drew it as such simply for convenience.

ACKNOWLEDGMENT

We thank Renjian Zheng for his assistance with molecular biology and Dr. Michele Sugantino for preparing Figure 1A.

REFERENCES

1. Williams, C. H., Jr. (1992) in *Chemistry and Biochemistry of Flavoenzymes* (Muller, F., Ed.) Vol. III, pp 121−211, CRC Press, Boca Raton.
2. Reed, L. J. (1974) *Acc. Chem. Res. 7*, 40−46.
3. Wierenga, R. K., Terpstra, P., and Hol, W. G. J. (1986) *J. Mol. Biol. 187*, 101−107.

4. Patel, M. P., and Blanchard, J. S. (1999) *Biochemistry 38*, 11827−11833.
5. Sakuda, S., Zhou, Z.-Y., and Amada, Y. (1994) *Biosci. Biotechnol. Biochem. 58*, 1347−1348.
6. Cole, S. T., Brosch, R., Parkhill, T. G., Churcher, C., Harris, D., Gordon, S. V., Eiglmeier, K., Gas, S., Barry, C. E., III, Tekaia, F., Badcock, K., Basham, D., Brown, D., Chillingworth, T., Connor, R., Davies, R., Devlin, K., Feltwell, T., Gentles, S., Hamlin, N., Holroyd, S., Hornsby, T., Jagels, K., Krogh, A., McLean, J., Moule, S., Murphy, L., Oliver, K., Osborne, J., Quail, M. A., Rajandream, M.-A., Rogers, J., Rutter, S., Seeger, K., Skelton, J., Squares, R., Squares, S., Sulston, J. E., Taylor, K., Whitehead, S., and Barrell, B. G. (1998) *Nature 393*, 537−544.
7. Smith, P. K., Krohn, R. I., Hermanson, G. T., Mallia, A. K., Gartner, F. H., Provenzano, M. D., Fujimoto, E. K., Goeke, N. M., Olson, B. J., and Klenk, D. C. (1985) *Anal. Biochem. 150*, 76−85.
8. Ottolina, G., Riva, S., Carrea, G., Danieli, B., and Buckmann, A. F. (1989) *Biochim. Biophys. Acta 998*, 173−178.
9. Orr, G., and Blanchard, J. S. (1984) *Anal. Biochem. 142*, 232−234.
10. Jencks, W. P., and Regenstein, J. (1976) in *Handbook of Biochemistry and Molecular Biology, Physical and Chemical Data* (Fasman, G. D., Ed.) Vol. I, 3rd ed., pp 338, CRC Press, Boca Raton.
11. Gerlt, J. A., and Babbitt, P. C. (2000) *Genome Biol. 1*, reviews 0005.1−0005.10.
12. Wilkinson, K. D., and Williams, C. H., Jr. (1981) *J. Biol. Chem. 256*, 2307−2314.
13. Wilkinson, K. D., and Williams, C. H., Jr. (1979) *J. Biol. Chem. 254*, 852−862.
14. Matthews, R. G., and Williams, C. H., Jr. (1976) *J. Biol. Chem. 251*, 3956−3964.
15. Benen, J., van Berkel, W., Dieteren, N., Arscott, D., Williams, C., Veeger, C., and de Kok, A. (1992) *Eur. J. Biochem. 207*, 487−497.
16. Rietveld, P., Arscott, L. D., Berry, A., Scrutton, N. S., Deonarian, M. P., Perham, R. N., and Willams, C. H., Jr. (1994) *Biochemistry 33*, 13888−13895.
17. Massey, V. (1960) *Biochim. Biophys. Acta 37*, 314−322.
18. Vienozinskis, J., Butkus, A., Cenas, N., and Kulys, J. (1990) *Biochem. J. 269*, 101−105.
19. Marcinkeviciene, J., and Blanchard, J. S. (1997) *Arch. Biochem. Biophys. 340*, 168−176.
20. Hopkins, N., and Williams, C. H. (1995) *Biochemistry 34*, 11757−11765.
21. Thorpe, C., and Williams, C. H., Jr. (1976) *J. Biol. Chem. 251*, 3553−3557.
22. Jarret, R. M., and Saunders, M. (1985) *J. Am. Chem. Soc. 107*, 2648−2654.
23. Karplus, P. A., and Schulz, G. E. (1987) *J. Mol. Biol. 195*, 701−729.
24. Lin, J., Westler, W. M., Cleland, W. W., Markley, J. L., and Frey, P. A. (1998) *Proc. Natl. Acad. Sci. U.S.A. 95*, 14664−14668.
25. Leichus, B. N., and Blanchard, J. S. (1992) *Biochemistry 31*, 3065−3072.
26. Wong, K. K., Vanoni, M. A., and Blanchard, J. S. (1988) *Biochemistry 27*, 7091−7096.
27. Patel, M. P., and Blanchard, J. S. (2001) *Biochemistry 40*, 5119−5126.
28. Leichus, B. N., Bradley, M., Nadeau, K., Walsh, C. T., and Blanchard, J. S. (1992) *Biochemistry 31*, 6414−6420.
29. Veine, D. M., Arscott, L. D., and Williams, C. H., Jr. (1998) *Biochemistry 37*, 15575−15582.
30. Massey, V., Gibson, Q. H., and Veeger, C. (1960) *Biochem. J. 77*, 341−351.
31. Matthews, R. G., Ballou, D. P., and Williams, C. H., Jr. (1979) *J. Biol. Chem. 254*, 4974−4981.
32. Thorpe, C., and Williams, C. H., Jr. (1981) *Biochemistry 20*, 1507−1513.
33. Matthews, R. G., Ballou, D. P., Thorpe, C., and Williams, C. H., Jr. (1977) *J. Biol. Chem. 252*, 3199−3207.
34. Mattevi, A., Obmolova, G., Sokatch, J. R., Betzel, C., and Hol, W. G. (1992) *Proteins 13*, 336−351.

BI010575O